Acta Cryst. (1985). B**41**, 161-169

Electron Rearrangement for the Water Molecule in Different Environments

BY KERSTI HERMANSSON*

Institute of Chemistry, Uppsala University, Box 531, *S*-751 21 *Uppsala, Sweden*

(*Received* 15 *March* 1984; *accepted* 15 *October* 1984)

Abstract

A series of *ab initio* SCF calculations has been made for the water molecule in various model complexes [$\oplus$.H_2O, $(H_2O)_2$, $H_2O.OH^-$, $Li^+.H_2O$, $(Li^+)_2.H_2O$, $(Li^+)_2(OH^-)_2.H_2O$] in different geometries to pinpoint specific electron rearrangement features for different water-molecule environments. Different types of neighbour give essentially the same electron redistribution in the H_2O molecule: an enhancement of the molecular dipole moment with electron depletion at the hydrogen sites and in the lone-pair region close to the oxygen nucleus, and an extended region of slight electron excess between the oxygen and the neighbouring cation or hydrogen-bond donor. For short contact distances there is an increase in the O lone-pair density both in $M^{n+}.H_2O$ complexes and $(H_2O)_2$. The nearest neighbours affect the H_2O deformation density in an approximately additive manner. Next-nearest neighbours cause in crystalline hydrates a substantial reduction of the deformation features. Very remote point charges, although large in number, have only a negligible effect on the H_2O electron density. A survey of experimentally determined electron density maps shows that experiment is generally not able to provide reliable information concerning intermolecular interactions for hydrates.

Introduction

Water is the molecule studied most extensively by diffraction techniques to date. The geometry and vibrational amplitudes of more than 250 crystallographically independent water molecules have been investigated by neutron diffraction; the number of X-ray diffraction studies is considerably larger. Improved experimental accuracy and computational facilities, and the development of more sophisticated scattering models now make it feasible to study finer detail in the electron distribution in crystals. Some twenty experimental electron density studies of crystalline hydrates have been published during the last decade. Substantial and, in many cases, significant differences are found between the various studies. In cases where the water-O atom is involved in an asymmetric bonding situation, for example, both larger and smaller lone-pair densities are observed in the direction of the shorter H···O contact. The present series of model calculations was undertaken to provide a tool for the interpretation of experimental electron density maps. Qualitative and quantitative features in the electron distributions are discussed. A comparison with experimentally determined densities is made.

Method

SCF calculations

Ab initio MO-LCAO-SCF calculations have been carried out for the H_2O molecule and for the H_2O complexes $\oplus.H_2O$, $Li^+.H_2O$, $(Li^+)_2.H_2O$, $(H_2O)_2$, $H_2O(OH^-)$ and $(Li^+)_2(OH^-)_2.H_2O$. The distances and angles between the coordinating species and the H_2O molecule have been varied, while the internal geometry of the H_2O molecule has been kept fixed (in most cases at 1·001 Å and 104·4°). No optimization of geometry has been performed; the main purpose is to show the electron redistribution within the H_2O molecule in the presence of an ion or a hydrogen-bonded H_2O molecule in different geometries.

The quantum-mechanical calculations were made with the program system *MOLECULE* (Almlöf, 1972). The basis sets consisted of contracted Gaussian-type functions. Dunning's (1970) $(9s5p)/\langle 4s2p\rangle$ set was used for O and his $(4s)/\langle 2s\rangle$ set for H, in both cases augmented with polarization functions according to Roos & Siegbahn (1970), *i.e.* a set of $3d$ functions with exponent 1·33 on O and a $2p$ (0·8) on H. For Li^+, the $(7s)/\langle 3s\rangle$ basis set was taken from Clementi & Popkie (1972) and the exponent of the $2p$ polarization function used (0·525) was derived by minimization of the energy of the $Li^+.H_2O$ complex. These basis sets were used for the calculation of all electron density maps, except those in Figs. 1(a)-1(c) and 9(e)-9(f).

For checking purposes, some of the deformation density maps were recalculated using larger basis sets, namely a $(10s6p1d)/\langle 5s3p1d\rangle$ set for O and $(5s1p)/\langle 3s1p\rangle$ for H (Dunning, 1971; Roos &

* Present address: IBM Corporation, Neighborhood Road, Kingston, New York 12401, USA.

0108-7681/85/030161-09$01.50

Siegbahn, 1970). Only very small changes in the deformation maps were observed. The basis set superposition error was checked using the counterpoise correction (Boys & Bernardi, 1970) and found to be insignificant.

The maps in Figs. 1(*a*)-1(*c*) have been calculated using the extended basis sets of Clementi & Popkie (1972) for O and H (except that no *f* functions were used on O), *i.e.* $(13s8p3d)/\langle 8s5p3d\rangle$ and $(6s2p1d)/\langle 4s2p1d\rangle$, respectively. The basis set used for Li was $(10s2p)/\langle 5s2p\rangle$ (Dunning, 1971). Fig. 1 allows a comparison between $\oplus.H_2O$ and $Li^+.H_2O$ complexes calculated with different basis sets. The deformation density in the $\oplus.H_2O$ complex in Fig. 1(*a*) shows the effect of polarization, while the calculation in Fig. 1(*b*), where 'empty' orbitals have been added at the $\oplus$ position, also allows charge transfer to take place. The deformation density of the $Li^+.H_2O$ complex in Figs. 1(*c*)-1(*d*) (calculated with different basis sets) includes polarization, charge transfer and exchange effects. The qualitative features of all four maps are similar, although the electron depletion close to the O atom is considerably smaller for the $Li^+.H_2O$ complex which includes effects of exchange interaction.

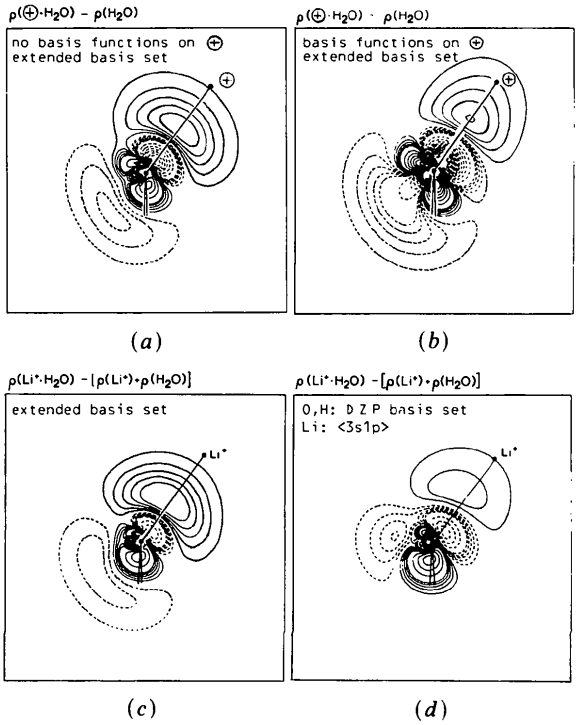

Fig. 1. Deformation electron density for an $\oplus.H_2O$ (*a*-*b*) and a $Li^+.H_2O$ (*c*-*d*) complex calculated with different basis sets. The cation position is at *B* in Fig. 6. The section shown is the plane bisecting the H-O-H angle. The H_2O geometry is 1·001 Å and 104·4° and the cation-O distance 2·00 Å. The basis sets used are indicated in the text. Contour levels at ±0·01, ±0·02, ..., ±0·05, ±0·10, ... e $Å^{-3}$. Positive contours (electron excess) are drawn as solid lines, negative contours (electron deficiency) are dashed, the zero contour is omitted.

Deformation maps

All deformation maps except those for the free H_2O molecule (Fig. 2) display a deformation of type

$$\delta\rho(\mathbf{r}) = \rho_{\text{complex}}(\mathbf{r}) - [\rho_{H_2O}(\mathbf{r}) + \rho_{\text{neighbours}}(\mathbf{r})]. \quad (1)$$

The geometry of the subtracted H_2O molecule is the same as that of the complex.

Note that two different sets of contour intervals have been used in the maps presented: ±0·01, ±0·02, ..., ±0·05, ±0·10, ... e $Å^{-3}$ and ±0·05, ±0·10, ... e $Å^{-3}$.

Results and discussion

Influence of internal geometry on the deformation density

An extensive survey of the geometry and environment of water molecules in crystalline hydrates has been made by Chiari & Ferraris (1982). In this survey, hydrogen bonds donated by water molecules in crystals were found to have O···O distances in the range 2·6-3·0 Å with an average value of 2·805 Å. For a hydrogen bond of length 2·6 Å, the O-H distance is approximately 0·04 Å longer than for a free water molecule, estimated on the basis of an empirical correlation between O-H and H···O distances (see *e.g.* Lundgren, 1974). The H-O-H angle varies between 100 and 114° (average value: 107·0°) in the hydrates studied by neutron diffraction (Chiari & Ferraris, 1982).

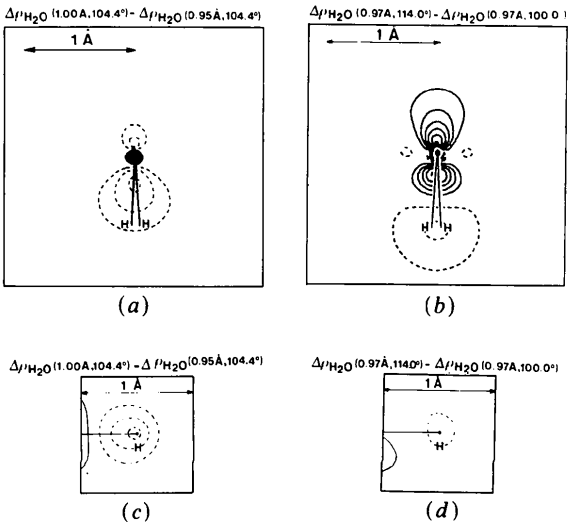

Fig. 2. Influence of the internal geometry on the deformation density of a free H_2O molecule. Here and in all following figures (except Figs. 9*e*-*f*) the basis sets used are the same as those in Fig. 1(*d*). Contour levels at ±0·05, ±0·10, ... e $Å^{-3}$. (*a*) Effect of different O-H distance; the section shown bisects the H-O-H angle; O atoms superimposed. (*b*) Effect of different H-O-H angles; same section as in (*a*); O atoms superimposed. (*c*) Effect of different O-H distance; section in the molecular plane; H atoms superimposed. (*d*) Effect of different H-O-H angles; same section as in (*c*); H atoms superimposed.

In experimentally determined deformation density maps the geometry used for the reference water molecule is usually the same as that in the crystal, although such maps neglect to display the electron rearrangement accompanying the change in the H_2O geometry compared to a non-bonded state. The electron redistribution due to intermolecular bonding of a free H_2O molecule can formally be written (here $\delta\rho$ denotes $\rho_{tot} - \sum \rho_{atoms}$):

$$\delta\rho_{complex}(\text{geom. 2}) - \delta\rho_{free\ H_2O}(\text{geom. 1})$$
$$\equiv [\delta\rho_{complex}(\text{geom. 2}) - \delta\rho_{free\ H_2O}(\text{geom. 2})] \quad \text{(i)}$$
$$+ [\delta\rho_{free\ H_2O}(\text{geom. 2}) - \delta\rho_{free\ H_2O}(\text{geom. 1})], \quad \text{(ii)}$$

where (i) is the electron redistribution for an H_2O molecule with the same geometry as in the bonded complex (crystal), and (ii) is the electron redistribution accompanying the change in geometry brought about by the environment.

If the effect of (ii) is small, it is possible to approximate the total electron redistribution by (i), which is also equivalent to $\rho_{complex}(\text{geom. 2}) - \rho_{free\ H_2O}(\text{geom. 2})$, *i.e.* is equivalent to (1).

The deformation electron density ($\rho_{tot} - \sum \rho_{atom}$) for a free H_2O molecule was calculated in different geometries corresponding to rather extreme variations [as judged from the survey by Chiari & Ferraris (1982)]. The resulting deformation maps look very similar for the H_2O geometries with O–H distances and H–O–H angles equal to (0·95 Å, 104·4°), (1·00 Å, 104·4°), (0·97 Å, 100·0°) and (0·97 Å, 114·0°), respectively (*cf.* also Hermansson, Olovsson & Lunell, 1984). Fig. 2 shows differences between these deformation maps; the O nuclei have been superimposed in Figs. 2(*a*)–2(*b*), the H nuclei in Figs. 2(*c*)–2(*d*). It is indeed seen that differences in the deformation density are generally quite small, but the changes around the H nuclei, for example, are as large as 0·15 e Å^{-3} for an O–H change of 0·05 Å. In such cases, however, the direct influence of the environment is also large. This is the case, for example, in an $Al^{3+}.H_2O$ complex with an Al^{3+}–O distance of 1·85 Å (Fig. 2*d* in Hermansson, Olovsson & Lunell, 1984). In order to describe the electron redistribution around the H nuclei correctly, the deficiency of −0·15 e Å^{-3} (Fig. 2*c* in the present paper) should be added to the deficiency of −1·0 e Å^{-3} (Fig. 2*d*, Hermansson, Olovsson & Lunell, 1984). The effect of changes in internal geometry on the electron distribution is neglected in the following discussion.

Effect of O-*atom neighbours*

The influence of one fixed-cation neighbour on the electron density of the H_2O molecule has been investigated by Hermansson, Olovsson & Lunell (1984) for the trigonal complexes $Li^+.H_2O$, $Be^{2+}.H_2O$, $Mg^{2+}.H_2O$ and $Al^{3+}.H_2O$ with M^{n+}–O distances chosen to correspond closely to those found in crystal structures. It was concluded that the *general features* of the H_2O deformation density are very similar in all these cases, even though the *magnitude* of the interaction depends on the charge of the cation and the cation–O distance. The main effect of the intermolecular interaction is to cause an electron flow

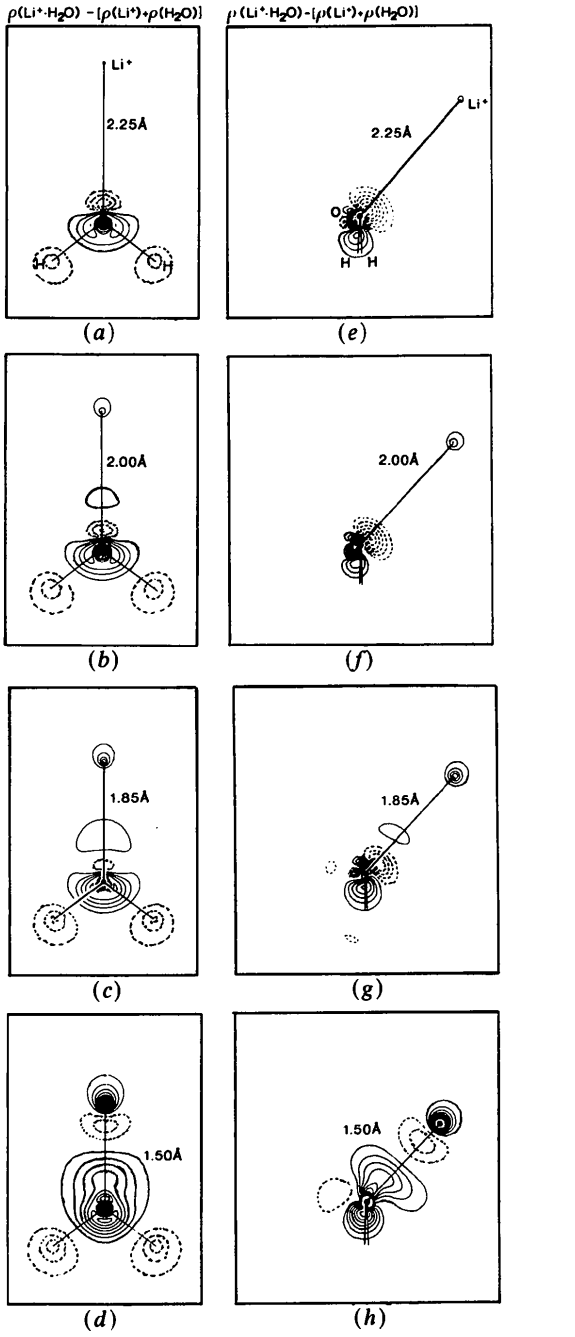

Fig. 3. Deformation electron density for $Li^+.H_2O$ complexes with different cation–O distances. The complexes in the left-hand column (*a*–*d*) are trigonal, while in the right-hand column (*e*–*h*) the Li^+ ion is situated in the plane bisecting the H–O–H angle. H_2O geometry: 0·957 Å, 106·5° in (*a*)–(*d*); 1·001 Å, 104·4° in (*e*)–(*h*). Contour levels at ±0·05, ±0·10, ... e Å^{-3}.

from the H towards the O atom, associated with an enhancement of the molecular dipole moment and an electron depletion at the H sites and in the O lone-pair region. There is also a weaker, extended region of electron excess between the O atom and its cation neighbours. The deformation densities for some $Li^+.H_2O$ complexes in different geometries are shown in Fig. 3 and for some $(H_2O)_2$ complexes in Fig. 4. The characteristics of the electron rearrangement caused by a hydrogen-bond-donating water neighbour at a distance close to the equilibrium geometry (Fig. 4*a*) are very similar to those observed for the cations above, although the features are weaker. Theoretical deformation maps of the type $\rho_{dimer} - \sum \rho_{monomers}$ have been published for several hydrogen-bonded dimers: H_2O (Diercksen, 1971; Yamabe & Morokuma, 1975), formamide (Dreyfus, Maigret & Pullman, 1970; Dreyfus & Pullman, 1970; Almlöf & Mårtensson, 1971*a*), formic acid (Almlöf & Mårtensson, 1971*b*; Eisenstein & Hirshfeld, 1983), acetic acid (Almlöf & Mårtensson, 1971*b*), formaldehyde-water (Yamabe & Morokuma, 1975). In all these cases one finds that the electron density is smaller in the O lone-pair lobe which accepts the hydrogen bond.

In the present calculations on $\oplus.H_2O$ and $Li^+.H_2O$, the cation–O distance was varied between 6·00 and 1·50 Å. Some of the $Li^+.H_2O$ complexes are shown in Fig. 3. The effect of different hydrogen-bond distances in the water dimer can be studied in Fig. 4; calculations with O···O distances up to 3·5 Å were performed, although all are not shown here. It would appear that, for long neighbour–O distances, a shortening of the bond leads to more pronounced density features. This is true in the whole range of distances between 6·00 and 1·50 Å for the $\oplus.H_2O$ complex, whereas for the $Li^+.H_2O$ complexes and the water dimers short neighbour–water distances lead to a more complex situation: below ~2·0 Å for the former and ~3·1 Å for the latter, the electron build-up in the intermolecular bond increases and moves closer to the O atom, while the electron-deficient region close to the O becomes smaller or disappears.*

The variation of the deformation density with cation–O distance is also shown quite clearly in Fig. 5, which displays the deformation electron density for two asymmetrical $(Li^+)_2.H_2O$ complexes. The standard deviations for good-quality experimental deformation electron density maps are often claimed to be of the order of 0·05 e $Å^{-3}$ in bonding regions. The deformation maps in Fig. 5 have been plotted

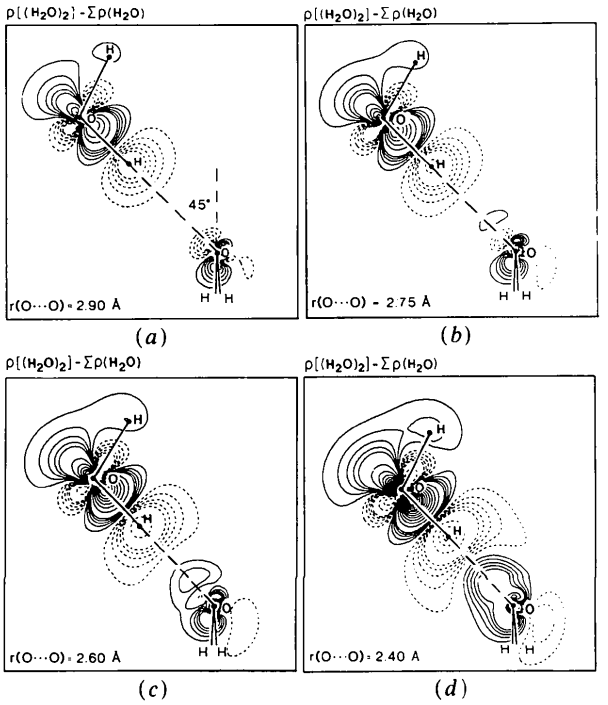

Fig. 4. Electron deformation density for some $(H_2O)_2$ model complexes with different O · · · O distances. The internal geometries of the two H_2O molecules have been kept fixed for both molecules (0·970 Å and 104·5° for the H-bond donating molecule, 0·970 Å and 105·0° for the H-bond accepting molecule). Contour levels at ±0·01, ±0·02, . . . , ±0·05, ±0·10, . . . e $Å^{-3}$.

* In this connection it could be mentioned that, within a project sponsored by the Commission on Charge, Spin and Momentum Densities of the International Union of Crystallography, four different experimental electron density studies have recently been carried out on α-oxalic acid.$2H_2O$ at low temperature (~100 K) (Coppens, 1984). All gave a consistent result concerning the distortion of the O lone-pair density from mirror-plane symmetry due to the presence of the incoming short hydrogen bond of 2·487 (1) Å (Feld & Lehmann, 1979). The dynamic *X–N* density is of the order of 0·05–0·10 e $Å^{-3}$ larger on the lone-pair side that accepts the hydrogen bond. This result implies, in fact, that the electron density excess arising from intermolecular interaction is here *larger* than 0·10 e $Å^{-3}$, since maps of the type $\rho_{tot} - \sum \rho_{atoms}$ display both the true intermolecular interaction and a lone-pair *decrease* due to a juxtaposition effect, *i.e.* an overlap of the deformation densities of unperturbed neighbouring molecules. The experimental electron excess is thus found to be larger than that expected from the theoretical result in Fig. 4.

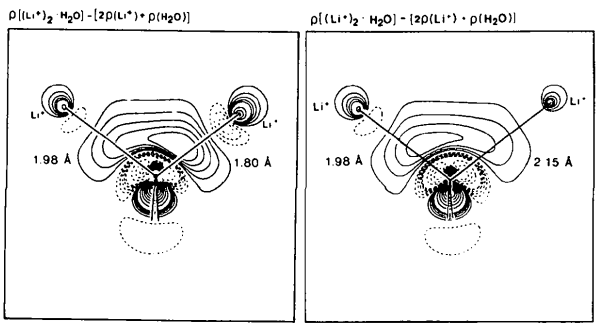

Fig. 5. Deformation electron density for two $(Li^+)_2.H_2O$ complexes. The Li^+–O–Li^+ plane makes an angle of 12° with the plane shown, which is the plane bisecting the H–O–H angle. H_2O geometry: 1·001 Å, 104·4°. Contour levels at ±0·01, ±0·02, . . . , ±0·05, ±0·10, . . . e $Å^{-3}$.

with rather small contour intervals (±0·01, ±0·02, ..., ±0·05, ±0·10, ... e Å^{-3}). Certain of the features in the figure (for example, the distinct asymmetry in the O lone-pair region) would thus not be observable in an X-ray diffraction experiment.

A comparison between Figs. 3 and 5 also shows that, to a first approximation, the deformation density features are additive. Actually, a calculation of the density $\rho[(Li^+)_2.H_2O] - \rho(Li^+.H_2O,\ 1{\cdot}85\ Å) - \rho(Li^+.H_2O, 1{\cdot}98\ Å) + \rho(H_2O)$ gives an almost featureless map: the largest peak is 0·06 e Å^{-3}; the density 0·20 Å from the O nucleus is 0·04 e Å^{-3}, and beyond 0·50 Å is less than 0·02 e Å^{-3}.

Figs. 6 and 7 display the dependence of the deformation density on the position of one cation neighbour at a fixed distance from the H_2O molecule. The positions *A* and *D* are both quite unrealistic cation positions; they are included only to display possible trends. The density in the lone-pair region is decreased on both sides of the H-O-H bisecting plane, even with only one cation neighbour present.

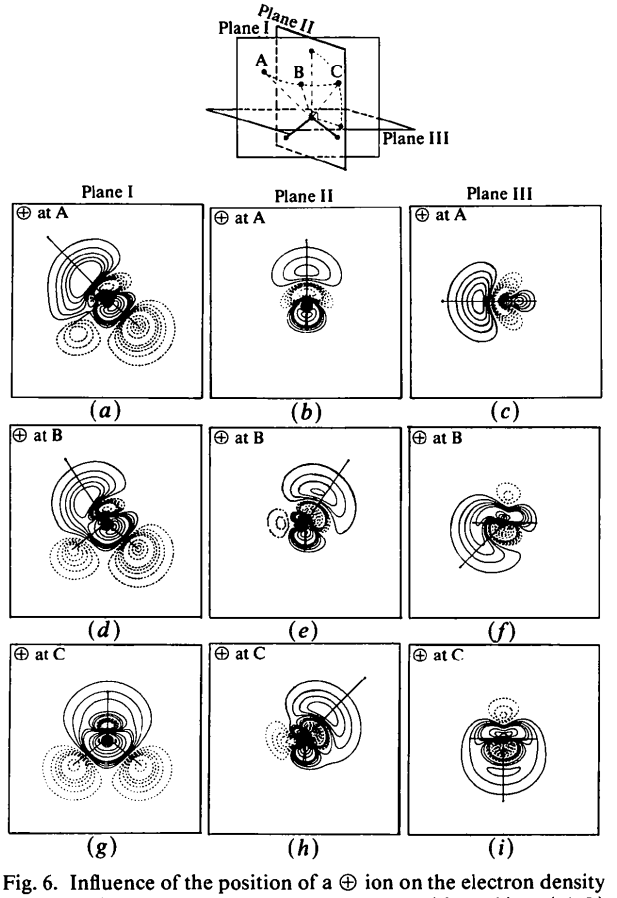

Fig. 6. Influence of the position of a ⊕ ion on the electron density of H_2O (lying in plane I). The maps show $\rho(\oplus.H_2O) - \rho(H_2O)$ in three different planes and for three different positions of ⊕ (*A*, *B*, *C*). The ⊕-O distances are all 2·00 Å. *A* is in plane I, *C* in plane II. Plane III is displaced 0·11 Å 'above' the O atom. H_2O geometry: 1·001 Å, 104·4°. Contour levels at ±0·01, ±0·02, ... ±0·05, ±0·10, ... e Å^{-3}.

The electron density decrease in the lone-pair region seems to be governed both by the 'direct' polarization towards the cation neighbour and by an internal electron rearrangement around the O atom which occurs when the electron density in the O-H bond is pulled towards the O atom. This electron migration along the easily polarizable O-H bonds causes a partial reversal of the electron redistribution which occurs when the free H_2O molecule is formed: in the free H_2O molecule, the electron excess in the lone-pair region occurs as a consequence of O-H bond formation; in the more nearly spherically symmetric environment of the crystal, the O lone pairs are reduced.

The existence of this internal rearrangement is supported by the deformation density maps in Fig. 8, where it is seen that the two positive neighbours situated at 45° to the H-O-H bisecting plane do not cause the density minima to lie in the O-⊕ directions (*cf.* the situation in $LiOH.H_2O$, especially Fig. 8*b* in Hermansson & Lunell, 1982). Instead, the positions of these minima seem to be governed by the internal symmetry of the H_2O molecule and the electron flow along the O-H bonds, as described above.

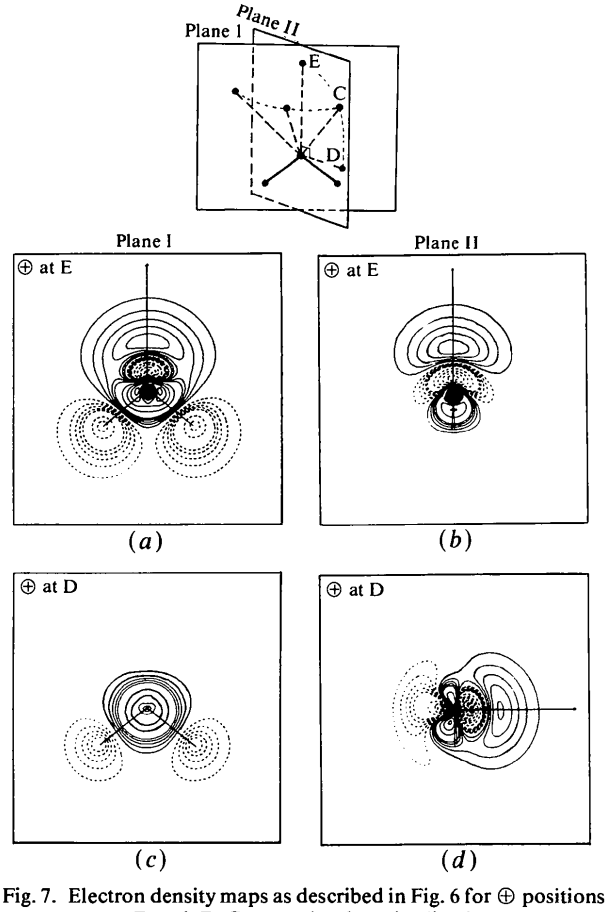

Fig. 7. Electron density maps as described in Fig. 6 for ⊕ positions *E* and *D*. Contour levels as in Fig. 6.

The deformation density is quite sensitive to a deviation of the cation position from the H-O-H bisecting plane. This is seen very clearly in Figs. 6(*a*) and 6(*d*) (and also in Fig. 9*a*) where the deformation features in the 'most favourably' directed O-H bond are much larger than in the other O-H bond.

Effect of hydrogen-bond acceptors

The deformation density for an H_2O molecule donating a hydrogen bond to another H_2O molecule is displayed in Fig. 4, and to an OH^- ion in Fig. 9(*c*). The influence of an F^- ion has been calculated by Diercksen & Kraemer (see Schuster, Jakubetz & Marius, 1975, and references therein). It can be seen that, in all these cases, the general features of the electron flow induced by the hydrogen-bond-accepting neighbours are very similar to those caused by cation neighbours on the O atom. Similarly, a comparison of Fig. 9(*d*) with Fig. 9(*b*) shows that, for the coordination geometry in $LiOH.H_2O$, the influence of the two OH^- ions on the deformation density of H_2O is very similar to that of the two Li^+ ions.

Effect of the total crystal environment

Fig. 9 shows the effect of the successive addition of nearest neighbours to the H_2O molecule in $LiOH.H_2O$. The effects appear approximately *additive*. This justifies the artificial decomposition of the effects of the intermolecular interaction into the fragmentary model complexes studied in the preceding sections. In contrast, intermolecular *interaction energies* are expected to show a significant component of non-additivity. So, for example, the interaction of the H_2O molecule in $LiOH.H_2O$ with its two Li^+ neighbours increases the polarity of the molecule [*cf.* Fig. 9(*b*)] and makes it a more efficient hydrogen-bond donor than a free H_2O molecule.

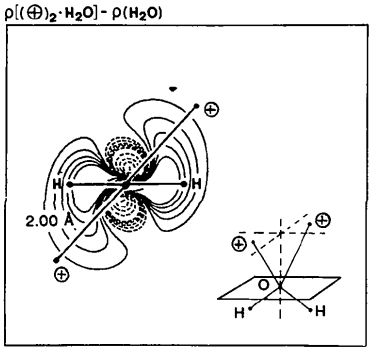

Fig. 8. Deformation electron density for a $\oplus_2.H_2O$ complex, where the angle between the $\oplus$-O-$\oplus$ plane and the plane bisecting the H-O-H angles is 45°. The section shown is perpendicular to the H-O-H bisector and 0·11 Å 'above' the O atom. H_2O geometry: 1·001 Å, 104·4°. Contour levels at ±0·01, ±0·02, ..., ±0·05, ±0·10, ... e Å^{-3}.

Calculations including only nearest neighbours (Fig. 9*e*) give a good description of general features and trends in the effect of intermolecular interaction on the water molecule in $LiOH.H_2O$. The total effect is severely exaggerated, however, compared to a true

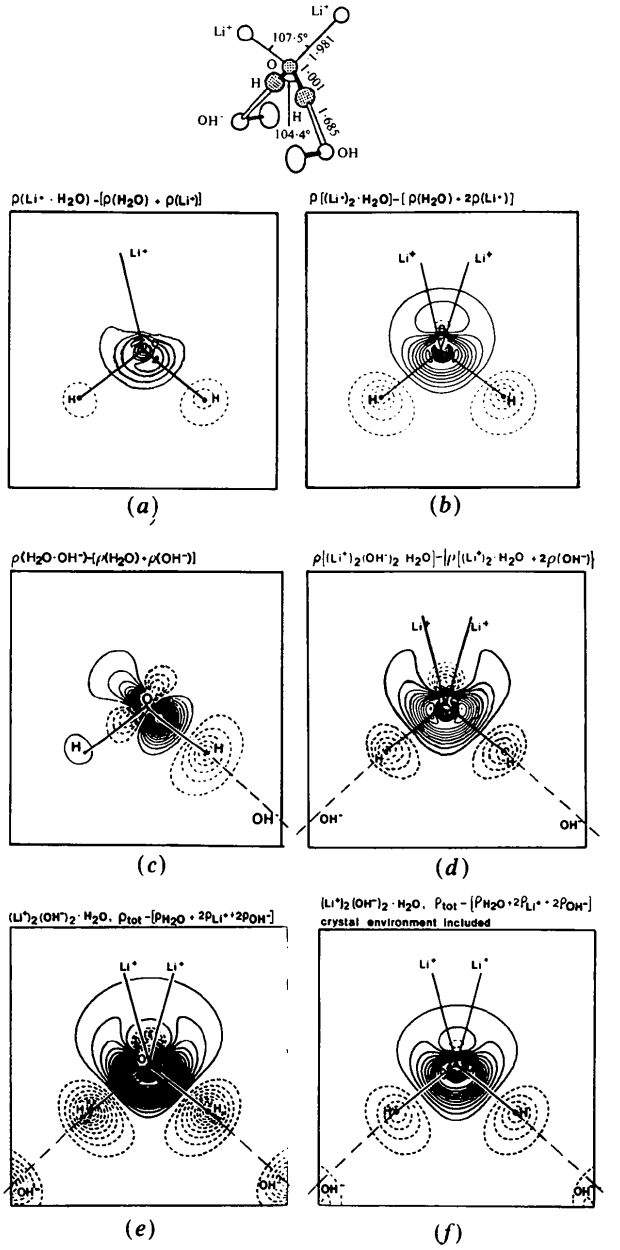

Fig. 9. The effect of the successive addition of nearest neighbours to the H_2O molecule in the $LiOH.H_2O$ crystal. The geometry of the $(Li^+)_2(OH^-)_2.H_2O$ complex is taken from the neutron diffraction study of $LiOH.H_2O$ (Hermansson & Thomas, 1982). The H_2O molecule lies on a twofold rotation axis; the O-H···O angle is 174·7°. The Li^+-O-Li^+ plane is twisted 12° with respect to the plane bisecting the H-O-H angle. The section shown is in the molecular plane. Basis sets in (*a*)-(*d*): same as in previous maps. Basis sets in (*e*)-(*f*): (10*s*6*p*1*d*)/⟨5*s*3*p*1*d*⟩ for water O, (5*s*1*p*)/⟨3*s*1*p*⟩ for water H and (10*s*1*p*)/⟨5*s*1*p*⟩ for Li (Dunning, 1971). Contour levels at ±0·05, ±0·10, ... e Å^{-3}. Distances in Å.

crystalline situation. When the rest of the crystalline environment is simulated by point charges (derived from a Mulliken population analysis), the deformation features decrease by about 50% (Fig. 9*f*).

The number of point charges included in Fig. 9(*f*) is 88 and corresponds to all neighbours within a radius of 5·8 Å from the water-O nucleus. As for the calculation of the *electrostatic potential*, this does not converge either when the number of point charges included in the $LiOH.H_2O$ calculation is increased by the successive increase of the radius of the limiting sphere, or when the central complex is surrounded by a large number of neutral unit cells (up to $39 \times 39 \times 39$ unit cells involving $1{\cdot}4 \times 10^6$ point charges). However, the effect on the magnitude of the potential of increasing the number of point charges (beyond those included in Fig. 9*f*) is constant (to 10%) within the van der Waals surface of the central water complex. It is also found that the potential, calculated in this way, differs by a constant value from the potential obtained by taking the whole crystalline environment into account using an Ewald (1921) summation according to the method of Bertaut (1952). However, since it is the *gradient* of the potential over the H_2O molecule which determines the electron flow within the molecule, the effect on the deformation density of the successive addition of more and more distant point charges around the central water molecule quickly becomes small. This is exemplified by a calculation including all neighbours within 10·0 Å from the central water O in $LiOH.H_2O$ [*i.e.* 561 point charges around the central $(Li^+)_2(OH^-)_2.H_2O$ complex]: the resulting density in the molecular plane differs by less than 0·09 e $Å^{-3}$ from that in Fig. 9(*f*).

Although the H_2O molecule in $LiOH.H_2O$ is strongly bonded, the effect of intermolecular interaction is modest (though not negligible). The theoretical calculations predict where we can expect to observe the effects of intermolecular bonding experimentally:

(i) The polarization of the water molecule leads to a decrease in the deformation density close to the H atoms which should be visible in experimental density studies, as indeed it is in $LiOH.H_2O$ (Fig. 3*a* in Hermansson & Thomas, 1982).

(ii) The major effects of intermolecular bonding on the lone-pair region occur close to the O nucleus; such effects may be difficult to observe experimentally.

(iii) The extended region of very low electron excess in the region between the H_2O oxygen and the cation neighbours would seem to be too weak to detect experimentally.

Several theoretical deformation density studies of varying quality have incorporated the crystalline environment as point charges in the calculations: α-glycine (Almlöf, Kvick & Thomas, 1973), uronium nitrate (de With, Feil & Baerends, 1975), $LiHCOO.H_2O$ (Thomas, Tellgren & Almlöf, 1975), $LiOH.H_2O$ (Hermansson & Lunell, 1982), NaHCOO (Fuess, Bats, Dannöhl, Meyer & Schweig, 1982), $LiNO_2.H_2O$ (Hermansson & Thomas, 1983) and $NaHC_2O_4.H_2O$ (Lunell, 1984). Van der Wal (1982) studied the effect of the crystalline environment on the H_2O molecule in $C_8H_{16}O_2.\frac{1}{2}H_2O$ with a model consisting of an H_2O molecule surrounded by four hydrogen-bonded CH_3OH molecules. Dannöhl, Meyer & Schweig (1980) have calculated the deformation density for the NaSCN crystal from the dynamically smeared theoretical deformation densities of free Na^+ and SCN^- ions. They have also calculated the effect of crystal field on the SCN^- density using a point-charge model for the nearest neighbours; this only led to changes of $<0{\cdot}05$ e $Å^{-3}$ in the electron density (Dannöhl, 1984) and produced no significant improvement in the agreement between the theoretical and experimental (Bats, Coppens & Kvick, 1977) maps.

The general conclusion from these studies is that the environment increases the polarity of the free molecules and that there is often a charge depletion in the O lone-pair region in H_2O or C–O groups. For the organic molecules listed above, the deformation changes due to the environment are small, often below 0·10 e $Å^{-3}$; the major changes here seem to occur in the π-bonding system (*cf.* Lunell, 1984). For the H_2O molecules in $LiNO_2.H_2O$, $LiHCOO.H_2O$, $C_8H_{16}O_2.\frac{1}{2}H_2O$ and, particularly, in $LiOH.H_2O$ and $NaHC_2O_4.H_2O$, the calculated effect of the crystalline environment on the static electron density is considerably larger.

Table 1 (left-hand side) is an attempt to summarize the results from these different theoretical calculations on H_2O and to obtain a quantitative estimate of the effects of intermolecular interaction on the deformation density for an H_2O molecule bound in a crystal. The effects of thermal smearing on the deformation density are estimated on the basis of the model calculations performed by Hermansson (1983).

The 'bound, stat.' peak heights and troughs are based on the calculations on $LiOH.H_2O$, $LiNO_2.H_2O$, $NaHC_2O_4.H_2O$ and $C_8H_{16}O_2.\frac{1}{2}H_2O$ (see earlier references). The 'bound, 300K' values are estimated on the basis of the calculations of the dynamic theoretical deformation density in the $LiOH.H_2O$ crystal (Schweig, 1983) and modified according to the following. The H_2O molecule in $LiOH.H_2O$ is particularly strongly bonded judging from the intermolecular bond distances, internal O–H distances, O–H stretching frequency (2775 cm^{-1} for the isotopically dilute HDO molecule) *etc.* In order to compensate for the fact that the vibrational amplitudes of the H_2O molecule are here particularly low, the values selected for the O–H and the O lone-pair peak heights in the 'bound, 300 K' case in Table 1 have been lowered by 0·05 e $Å^{-3}$ from the values for the dynamic theoretical deformation density in

Table 1. *Typical peak heights and troughs* (e Å^{-3}) *for the deformation density* ($\rho_{tot}-\sum_{atom\ i}\rho_i$) *of the free and bound* H_2O *molecule*

	Theoretical					Experimental	
	free			bound		bound	
	stat.[a]	100 K[b]	300 K[b]	stat.[c]	300 K[d]	stat.[e]	100 K[f]
O–H	0·60	0·35	0·25	0·60	0·25	0·65	0·25–0·45
O lone pair	1·40	0·55	0·40	1·00	0·35	0·20	0·20–0·35
H nuclei	0·40	0·25	0·15	0·10	0·00	0·00	0·00–0·20
'Outside' H	−0·20	−0·15	−0·10	−0·25	−0·15	−0·25	−0·05–−0·15

(*a*) See *e.g.* Fig. 6 in Hermansson & Lunell (1982).
(*b*) Rigid-body vibrations of a bound H_2O molecule in a crystal have been applied to the free-molecule deformation density (Hermansson, 1983).
(*c*) Estimate based on calculations on $LiOH.H_2O$, $LiNO_2.H_2O$, $NaHC_2O_4.H_2O$, and $C_8H_{16}O_2.\frac{1}{2}H_2O$ (see text).
(*d*) Estimate based on results for $LiOH.H_2O$ (see text).
(*e*) From Hermansson & Thomas (1982).
(*f*) See text.

$LiOH.H_2O$. The difference between the theoretical deformation for the 'free, 300 K' and the 'bound, 300 K' cases in Table 1 should thus provide an estimate of the upper limit for the magnitude of the effects of intermolecular interaction on the room-temperature dynamic deformation density of an H_2O molecule in a crystal. The theoretical calculations thus show that the intermolecular influence on the *static* deformation density is expected to be $\leq 0{\cdot}40$ e Å^{-3} in the O lone-pair region and $\leq 0{\cdot}30$ e Å^{-3} in the O–H bond regions and at the H positions, while the intermolecular influence on the *dynamic* deformation density (at room and low temperature) is $\leq 0{\cdot}15$ e Å^{-3}. It can also be noted that differences of the order of 0·05 e Å^{-3} for the room-temperature deformation density may be expected for H_2O molecules in distinctly different bonding situations, simply due to different vibrational amplitudes.

Comparison with experimental deformation densities

Some twenty hydrates have been studied to date by $X-N$, $X-X_{high}$ or multipole refinement techniques. The deformation density maps for the H_2O molecules in these different hydrates show a variation which is much larger than can reasonably be expected to arise from the influence of different bonding environment or different thermal motion. Unfortunately, many of the deformation densities display physically quite unrealistic features, and it must be concluded that the densities for these H_2O molecules are subject to large errors. This leaves only a handful of compounds available for the discussion of trends in bonding features, namely $C_8H_{16}O_2.\frac{1}{2}H_2O$ (86 K; van der Wal, 1982), α-$H_2C_2O_4.2H_2O$ (100 K; Stevens & Coppens, 1980), $LiNO_3.3H_2O$ (120 K; Hermansson, Thomas & Olovsson, 1984), $LiOH.H_2O$ (295 K; Hermansson & Thomas, 1982), $MgSO_3.6H_2O$ (120 K; Bats, Fuess & Elerman, 1984), $MgS_2O_3.H_2O$ (120 K; Elerman, Bats & Fuess, 1983) and $NaHC_2O_4.H_2O$ (120 K; Delaplane, Tellgren & Olovsson, 1984).

The peak heights and troughs for the low-temperature deformation density studies above are summarized in the 'Experimental, 100 K' column in Table 1. On the basis of the theoretical results in Table 1, and estimating the variation of the dynamic deformation density with temperature from the corresponding variation for the free H_2O molecule ('free, stat.', 'free, 100 K', 'free, 300 K'), it can be concluded that the experimental deformation features in the O–H region and at the H positions are in good agreement with theoretical prediction. In the lone-pair O region, however, the experimental density generally appears too low. This circumstance has its origin in the limited $\sin\theta/\lambda$ cut-off in an X-ray diffraction experiment and the lower relative accuracy of the measured high-order intensities; as a result, no reliable information can be obtained about the sharp electron density features close to the non-hydrogen nuclei. Although the discrepancy is much more pronounced when *static* experimental and theoretical electron densities are compared, it is evident also for the *dynamic* densities.

Inspection of the experimental deformation densities for the H_2O molecules listed above reveals no trends with respect to the variation of the deformation density features with different bonding environment. It was stated above that the dynamic deformation density peak heights are expected to differ by $<0{\cdot}15$ e Å^{-3} for a free and a bonded H_2O molecule. The variation between different crystalline bonding situations should be even smaller. In view of the relatively small number of accurate electron density studies of hydrates that have been performed, and in view of the fact that the precision in these deformation densities is generally not better than 0·05 e Å^{-3}, it must be concluded that significant trends are not expected to be clearly exposed. A larger number of more accurate studies is needed before the effects of intermolecular bonding can be discussed on the basis of experiment. To achieve this end, an increase in the overall precision of the experimental data is essential, as well as a more appropriate treatment of basic

scattering phenomena. The latter would involve the development of better and more readily applicable models for treating, for example, thermal diffuse scattering, and a more general willingness to take the trouble to apply these models routinely.

I wish to thank Professor Ivar Olovsson for his support and interest in this work. Financial support from the Swedish Natural Science Research Council is also gratefully acknowledged.

References

ALMLÖF, J. (1972). USIP Report 72-09. Univ. of Stockholm.
ALMLÖF, J., KVICK, Å. & THOMAS, J. O. (1973). *J. Chem. Phys.* **59**, 3901-3906.
ALMLÖF, J. & MÅRTENSSON, O. (1971*a*). *Acta Chem. Scand.* **25**, 355-356.
ALMLÖF, J. & MÅRTENSSON, O. (1971*b*). *Acta Chem. Scand.* **25**, 1413-1417.
BATS, J. W., COPPENS, P. & KVICK, Å. (1977). *Acta Cryst.* B**33**, 1534-1542.
BATS, J. W., FUESS, M. & ELERMAN, Y. (1984). To be published.
BERTAUT, E. F. (1952). *J. Phys. Radium*, **13**, 499.
BOYS, S. F. & BERNARDI, F. (1970). *Mol. Phys.* **19**, 553-566.
CHIARI, G. & FERRARIS, G. (1982). *Acta Cryst.* B**38**, 2331-2341.
CLEMENTI, E. & POPKIE, H. (1972). *J. Chem. Phys.* **57**, 1077-1094.
COPPENS, P. (1984). *Acta Cryst.* A**40**, 184-195.
DANNÖHL, H. (1984). Private communication.
DANNÖHL, H., MEYER, H. & SCHWEIG, A. (1980). *Chem. Phys. Lett.* **69**, 75-77.
DELAPLANE, R. G., TELLGREN, R. & OLOVSSON, I. (1984). To be published.
DIERCKSEN, G. H. F. (1971). *Theor. Chim. Acta*, **21**, 335-367.
DREYFUS, M., MAIGRET, B. & PULLMAN, A. (1970). *Theor. Chim. Acta*, **17**, 109-119.
DREYFUS, M. & PULLMAN, A. (1970). *Theor. Chim. Acta*, **19**, 20-37.
DUNNING, T. H. (1970). *J. Chem. Phys.* **53**, 2823-2833.
DUNNING, T. H. (1971). *J. Chem. Phys.* **55**, 716-723.
EISENSTEIN, M. & HIRSHFELD, F. L. (1983). *Acta Cryst.* B**39**, 61-75.
ELERMAN, Y., BATS, J. W. & FUESS, H. (1983). *Acta Cryst.* C**39**, 515-518.
EWALD, P. P. (1921). *Ann. Phys. (Leipzig)*, **64**, 253.
FELD, R. & LEHMANN, M. S. (1979). Unpublished results.
FUESS, H., BATS, J. W., DANNÖHL, H., MEYER, H. & SCHWEIG, A. (1982). *Acta Cryst.* B**38**, 736-743.
HERMANSSON, K. (1983). *Chem. Phys. Lett.* **99**, 295-300.
HERMANSSON, K. & LUNELL, S. (1982). *Acta Cryst.* B**38**, 2563-2569.
HERMANSSON, K., OLOVSSON, I. & LUNELL, S. (1984). *Theor. Chim. Acta*, **64**, 265-276.
HERMANSSON, K. & THOMAS, J. O. (1982). *Acta Cryst.* B**38**, 2555-2563.
HERMANSSON, K. & THOMAS, J. O. (1983). *Acta Cryst.* C**39**, 930-936.
HERMANSSON, K., THOMAS, J. O. & OLOVSSON, I. (1984). *Acta Cryst.* C**40**, 335-340.
LUNDGREN, J.-O. (1974). *Acta Univ. Ups.* No. 271.
LUNELL, S. (1984). *J. Chem. Phys.* **80**, 6185-6193.
ROOS, B. & SIEGBAHN, P. (1970). *Theor. Chim. Acta*, **17**, 199-208.
SCHUSTER, P., JAKUBETZ, W. & MARIUS, W. (1975). *Top. Curr. Chem.* **60**, 1-108.
SCHWEIG, A. (1983). Private communication.
STEVENS, E. D. & COPPENS, P. (1980). *Acta Cryst.* B**36**, 1864-1876.
THOMAS, J. O., TELLGREN, R. & ALMLÖF, J. (1975). *Acta Cryst.* B**31**, 1946-1955.
WAL, R. J. VAN DER (1982). Thesis. Univ. of Groningen.
WITH, G. DE, FEIL, D. & BAERENDS, E. J. (1975). *Chem. Phys. Lett.* **34**, 497-499.
YAMABE, S. & MOROKUMA, K. (1975). *J. Am. Chem. Soc.* **97**, 4458-4465.

Acta Cryst. (1985). B**41**, 169-172

A Molecular-Packing Analysis of the Crystal Structures of Ice

BY DAVID HALL AND MURRAY K. WOOD

Chemistry Department, University of Auckland, New Zealand

(*Received* 16 *July* 1984; *accepted* 7 *November* 1984)

Abstract

A rationalization of the structures of the crystalline phases of ice has been attempted, through lattice-energy calculations based upon the ST2 potential model for interaction between water molecules. Ordered models for H-atom coordinates were assumed, where these are not experimentally available. Calculated energies were broadly consistent with the phase diagram, except for ice I and ice V which both calculate as being more stable than is observed. The calculated energy for ice VIII is highly dependent upon the relative directions of the polarity of the two independent hydrogen-bond networks.

Introduction

It has been demonstrated in a number of studies of the crystal structures of rigid molecules (Kitaigorodskii, 1970; Williams & Starr, 1977) that the observed structure corresponds to those values of the cell and molecular parameters for which lattice energy is a minimum. Such studies normally assume knowledge of the space group and the number of molecules per cell, and only in that limited sense could they be described as having predicted the crystal structure. Prediction without such restriction on the basis of calculated energy alone would be a formidable computational task, and has only been attempted in

0108-7681/85/030169-04$01.50